TESTING THE HYDRODYNAMIC BEHAVIOR OF A LOAM SOIL BY BEERKAN INFILTRATION RUNS WITH SIX HEIGHTS OF WATER POURING

M. Castellini[1,*], M. Iovino[2], V. Bagarello[2]

[1] Council for Agricultural Research and Economics–Research Center for Agriculture and Environment (CREA–AA), Via C. Ulpiani 5, Bari 70125, Italy
[2] Department of Agricultural, Food and Forest Sciences, University of Palermo, Viale delle Scienze, Building No. 4, 90128 Palermo, Italy

*Corresponding author.
E-mail address: mirko.castellini@crea.gov.it (M. Castellini).

ABSTRACT

Interpreting and simulating rainfall partition into infiltration and surface runoff has to consider that surface soil hydraulic properties, including saturated soil hydraulic conductivity (K_s) and sorptivity (S), could change even at very short temporal scales. Soil deterioration due to water impact can be tested in the field by the multi-height beerkan (MHB) method, that is, by pouring water on the infiltration surface from different heights. Soil hydraulic properties can be estimated coupling the MHB method with the BEST-steady algorithm. The MHB method with six heights of water pouring (H) in the range 0.03-2 m was applied on a relatively dry loam soil to investigate height of water pouring effects on i) the established infiltration process, and ii) K_s, S, the scale parameter of the water retention curve (h_g) and the characteristic microscopic pore radius (λ_m). Higher heights of water pouring generally induced a slowdown of the infiltration process, smaller S, K_s and λ_m values and higher $|h_g|$ values. The S, K_s, $|h_g|$ and λ_m vs. H relationships were statistically significant but the fitted relationships for S and K_s were stronger than those for $|h_g|$ and λ_m, indicating a different sensitivity of the considered parameters to the height of water pouring. Small or negligible soil deterioration was observed for both small ($H \leq 0.25$ m) and large ($H \geq 1.5$ m) heights. Between these two extremes, the soil deteriorated as H increased, suggesting that the external solicitations were high enough to overcome the resistance of the porous medium but not so high to determine a complete soil alteration. The tested methodology appears promising to determine the effects of water impact on the soil hydrodynamic behavior and it could be applied to perform a soil hydraulic characterization usable for modelling hydrological processes.

Keywords: surface hydrological processes; soil hydraulic properties; soil deterioration; multi-height beerkan method.

INTRODUCTION

Interpreting and simulating rainfall partition processes into infiltration and surface runoff is an open topic in hydrological sciences and it is essential to quantify the agro-environmental impacts on water storage, soil loss and fertility, which are causing growing concerns due to the ongoing climate changes (Assouline and Mualem, 2002, 2006; Chen et al., 2013).

Surface soil hydraulic properties, including saturated soil hydraulic conductivity (K_s) and sorptivity (S) that have a direct impact on infiltration (Philip, 1957; Parlange et al., 1982; Haverkamp et al., 1994), can change even at very short temporal scales, such as during a rainfall event or between closely spaced rainstorms (Fohrer et al., 1999; Mügler et al., 2019; Ndiaye et al., 2005). The highly dynamic nature of the upper soil layer makes description of changes of structure dependent soil hydraulic properties necessary but very complex

(Somaratne and Smettem, 1993; Ndiaye et al., 2005; Todisco et al., 2023). The reason is that many factors influence surface soil changes, including the characteristics of the rainfall events, the soil type and the soil conditions at the time of the event. Moreover, different soil properties can exhibit different degrees of variation, depending on the particular context. For example, changes in the soil hydraulic properties following soil tillage were investigated in rainfall simulation trials of intermittent rain by Todisco et al. (2023). During a sequence of wetting and drying cycles, S and K_s decreased by 2.9–3.1 and 1.4–2.2 times, respectively, depending on the plot, with a more evident decline for S than for K_s. In other investigations, however, the suggestion was that K_s should be considered as a sort of sentinel property, due its high sensitivity to water impact application procedures (Auteri et al., 2020; Castellini et al., 2021a). Moreover, Bagarello et al. (2023) recently showed that disturbance effects change with the initial soil moisture and structural conditions, as they were relatively small when the soil was relatively little sorptive and conductive, but they became noticeable in the opposite condition. Therefore, it can be expected that initially drier soils can be more sensitive to rainfall induced soil disturbance than wetter soils (Martínez-Mena et al., 1998; Fohrer et al., 1999).

Development of simple experimental methods to determine directly in the field changes in soil hydraulic properties in a wide range of hydrologically relevant scenarios could help to obtain a more realistic soil hydraulic characterization for simulating hydrological processes.

The effects of soil deterioration due to water pouring from different heights can be tested in the field by an adapted single-ring infiltrometer method introduced by Bagarello et al. (2014a), and recently called "multi-height beerkan", MHB, method (Castellini et al. 2021a). Soil hydraulic properties can be determined from MHB experiments by the so-called BEST (Beerkan Estimation of Soil Transfer parameters)-steady algorithm (Bagarello et al., 2014b). The classical beerkan experiment (Lassabatere et al., 2006), i.e., an infiltration experiment in which the disturbance of the surface soil layer is practically negligible, is expressive of the overall effect on infiltration rate of different factors such as hydraulic potential gradient, wetting induced swelling, mechanical impact of the poured water, mobilization of soil particles released by slaking and weakening of the interparticle bonds. Instead, an infiltration experiment in which water is poured by a non-zero height should be expressive of the effect of the same factors plus the additional mechanical impact of the applied water on the soil surface (Auteri et al., 2020). The MHB method was i) successfully validated by comparison with the classical rainfall simulator method (Di Prima et al., 2017); ii) used with relatively large infiltration surfaces, presumably yielding more representative data than small surfaces (Castellini et al., 2021a); iii) applied to estimate the effects of the height of water pouring on the surface soil physical quality (Castellini et al., 2021b); and iv) used to study the soil response to continuous (Bagarello et al., 2023) or intermittent (Alagna et al., 2018; Bagarello et al., 2020) water pouring sequences, Therefore, the usability of the MHB method to obtain soil data specifically representative of an altered surface soil layer was demonstrated. It is still unclear if this method, perhaps with some adaption, is also usable to obtain relevant soil data for simulating hydrological processes.

Previous investigations have used two or three heights of water pouring (e.g., Bagarello et al., 2014a; Auteri et al., 2020; Castellini et al., 2021a). However, considering more heights of water pouring could yield a more complete information on changes in soil hydraulic properties as a consequence of water mechanical impact on the infiltration surface. For example, it could be established if there is a minimum water height below which the soil resists mechanical impact or, at the other extreme, a maximum water height above which soil hydraulic properties do not change further. Furthermore, the shape of the relationship between the soil hydraulic properties and the height of water pouring could be determined with some confidence. Taking into account that changing the height of water pouring means varying the

impact energy of the applied water, such relationships could represent at least the starting point of a more accurate description of soil hydrodynamic response in models that simulate surface soil hydrological processes.

The main objective of this study was to test the MHB method using six heights of water pouring. A relatively dry loam soil was sampled to i) verify height of water pouring effects in the rather wide range of 0.03 m to 2 m on the established infiltration process; and ii) establish in detail water pouring height effects on saturated soil hydraulic conductivity, soil sorptivity, scale parameter of the water retention curve and characteristic microscopic pore radius.

MATERIALS AND METHODS

Field site

The investigation was carried out in an undisturbed fallow plot of about 200 m^2, established at the experimental field of the Council for Agricultural Research and Economics, Research Center for Agriculture and Environment (CREA-AA) of Bari, Italy (41˚06′37.31″ N, 16˚52′40.12″ E). According to the USDA classification system, the soil was loam, with 43.2% of sand and 17.2% of clay (Castellini et al., 2021a). The field campaign was performed in nearly 40 days, during the spring-summer season of 2022. No appreciable rainfall events occurred during this period.

Experiment

Single-ring infiltration runs of the beerkan type (Lassabatere et al., 2006) were carried out at randomly selected locations by pouring water on the soil surface from six different heights, H (L). In particular, water was applied from approximately 0.03 (H0.03), 0.25 (H0.25), 0.5 (H0.5), 1 (H1), 1.5 (H1.5) and 2 (H2) m (**Fig. 1**). For each H value, the infiltration run was replicated ten times, yielding a total of 60 runs. Plexiglas tubes of the same diameter as the ring and of fixed heights were positioned over the ring during the run to ensure flow verticality and prevent possible deviations of the poured water due to wind.

At a sampling point, the herbaceous vegetation was removed by scissors leaving the roots in situ. A metal ring with an inner diameter equal to 15 cm was inserted 1 cm into the soil to avoid lateral loss of water (Lassabatere et al., 2006). For a given run, 15 water volumes, each of 200 mL, were poured without interruption on the confined infiltration surface. In particular, a given volume of water was poured in the ring in approximately 3-5 s at the start of the run and the elapsed time during its infiltration was measured. When the amount of water had completely infiltrated, an identical amount of water was poured into the ring, and the time needed for water to infiltrate was logged. Finally, 15 cumulative infiltration, I (L), vs. time, t (T), data points were determined to describe a cumulative infiltration curve.

For each run, an undisturbed soil core (10 cm in height by 5 cm in diameter) was collected at the 0 to 10 cm depth no farther than about 5-10 cm from the wetted zone. These soil cores were used to determine the dry soil bulk density, ρ_b, and the soil water content at the time of sampling, θ_i. Therefore, a ρ_b and a θ_i dataset were developed for each H value. The saturated soil water content, θ_s, was assumed to coincide with the soil porosity, f, assuming a soil particle density of 2.65 g/cm^3 (Mubarak et al., 2009).

Calculations and data analysis

Initially, the infiltration data were reported on cumulative infiltration, I (L), vs. time, t (T), and infiltration rate, i_r (L/T), vs. I plots to take an initial look at the general response of the different types of experiments (H0.03, H0.25, H0.5, H1, H1.5 and H2). The i_r vs. I plot was considered since durations changed with the run, making presentation of all data on a single i_r vs. t plot rather confuse.

For a given height of water pouring, the mean infiltration time, Δt (T), of each applied water volume (1^{st}, 2^{nd}, …, 15^{th}) was calculated. The ratio between the mean of Δt for a given H, with $H > 0.03$ m, Δt_H, and the corresponding mean of Δt for $H = 0.03$ m, $\Delta t_{0.03}$, was then plotted against the number of the applied water volumes, n_v, to detect the effect of the height of water pouring on the established infiltration process. The premise was that $\Delta t_{0.03}$ was expressive of the overall effect on infiltration rate of different factors such as hydraulic potential gradient, wetting induced swelling, mechanical impact of the poured water, mobilization of soil particles released by slaking and weakening of the interparticle bonds. The Δt_H value expressed the effect of the same factors plus the additional water mechanical impact on the soil surface due to application of water from a higher height. Therefore, a $\Delta t_H/\Delta t_{0.03}$ value equal to one denoted that the height of water pouring did not have any effect on the infiltration process whereas a value greater than one indicated that the height of water pouring induced a slower infiltration process. For a given $\Delta t_{0.03}$ value, higher $\Delta t_H/\Delta t_{0.03}$ ratios signaled larger differences between high ($H > 0.03$ m) and low ($H = 0.03$ m) runs.

The BEST-steady algorithm, that uses the intercept, b_s (L), and the slope, i_s (L/T), of the straight line fitted to the last data points describing steady-state conditions on the I vs. t plot (Bagarello et al., 2014b), was selected to determine the soil hydrodynamic properties. This choice was made since, in other investigations, BEST-steady allowed a successful treatment of runs involving soil alteration and led to saturated soil hydraulic conductivity values close to those obtained by rainfall simulation (Di Prima et al., 2018). Moreover, this algorithm was considered more appropriate than other BEST algorithms (BEST-slope by Lassabatere et al., 2006 and BEST-intercept by Yilmaz et al., 2010) to capture the overall effects of possible soil alteration phenomena occurring during infiltration. Although steady-state conditions have to be attained to calculate soil hydrodynamic parameters with any BEST algorithm, BEST-steady only requires data for the final stage of the run while BEST-slope and BEST-intercept combine an information collected at the end of the run (i_s; all possible alteration has occurred) with transient infiltration data (alteration is likely occurring).

For this investigation, involving an intentional modification of soil surface conditions, it was preliminarily tested if 15 water volumes were enough to achieve steady-state conditions during the established infiltration processes. At this aim, the empirical Horton (1940) infiltration model was fitted to the data for each field run. This model describes infiltration using three parameters, that is initial infiltration rate (at time $t = 0$), i_{0H} (L/T), final infiltration rate, i_{fH} (L/T), and a decay constant, k_H (1/T), denoting the rate at which i_{0H} approaches i_{fH}. A comparison was then established between i_{fH} and the i_s values estimated from the last three (I, t) data points (Castellini et al., 2021a). Obtaining $i_s \approx i_{fH}$ was considered to support, or at least not to evidently refute, the reliability of the estimated i_s and the associated b_s values. Instead, $i_s > i_{fH}$ was viewed as a sign of a likely overestimation of steady-state infiltration rate. To support this reasoning, **Fig. 2** shows an example for a Horton infiltration process with known parameters. Applying the Horton model to a short run did not compromise estimation of the true final infiltration rate that was instead overestimated by linear regression of the last three (I, t) data points.

Saturated soil sorptivity, S (mm/h$^{0.5}$), saturated soil hydraulic conductivity, K_s (mm/h), and the scale parameter of the water retention curve by van Genuchten (1980), h_g (mm) (Lassabatere et al., 2006), were then determined for each run with BEST-steady. The macroscopic capillary length (White and Sully, 1987) was also determined from b_s and $\Delta\theta = \theta_s - \theta_i$ according to Di Prima et al. (2020). The characteristic microscopic pore radius, λ_m (mm), of the soil was then calculated using this characteristic length (White and Sully, 1987).

The distribution of the data obtained with different heights of water pouring was checked with the Lillefors (1967) test at $P = 0.05$, considering both a normal (NO) and a ln-normal (LNO) distribution. Regardless of H, the NO distribution hypothesis was never rejected for S, K_s and

$|h_g|$. Therefore, the arithmetic mean and the associated coefficient of variation, *CV*, were used to summarize these data as well as the ρ_b and θ_i data, in accordance with other investigation (e.g., Mubarak et al., 2009). With reference to λ_m, only the LNO distribution hypothesis was not rejected for the six developed datasets. In this case, the data were summarized by the geometric mean and the associated *CV* (Lee et al., 1985).

A pairwise approach was applied to compare runs differing by the height of water pouring. A pairwise approach was preferred over a multiple comparison approach because comparing the results for, e.g., H = 0.03 m and H = 0.5 m was considered not to depend on the data collected with other heights of water pouring (e.g., H = 2 m). Therefore, F and two-tailed, unpaired t tests were applied to the untransformed ρ_b, θ_i, S, K_s and $|h_g|$ data and to the ln-transformed λ_m data since the infiltration runs were performed at different locations of the field site.

Regression analyses between soil hydrodynamic parameters and H were performed by considering the exponential, linear, logarithmic and power relationships and retaining the relationship having the highest coefficient of determination, R^2, for further analysis. The choice to consider different relationships was made since the shape of the tested relationships was not predictable in advance. A two-tailed t test was also used to establish the statistical significance of a fitted regression line to the data (Glantz, 2012). All statistical tests were carried out at P = 0.05.

RESULTS

Dry soil bulk density and antecedent soil water content

Sites sampled with different H values had mean dry soil bulk density values that varied from 1.22 g/cm^3 to 1.29 g/cm^3, that is by 5.7% at the most (**Table 1**). Differences were significant for only one of the 15 established comparisons, i.e. with reference to the comparison between the ρ_b values corresponding to H = 0.25 m and H = 2 m. Relative variability of ρ_b was small for each dataset ($CV \leq$ 7.9%), as expected for this soil property (Warrick, 1998).

The mean antecedent soil water content values varied between 0.155 m^3/m^3 and 0.173 m^3/m^3, that is by no more than 11.6%. Significant differences were detected in three cases, that is for the comparisons between θ_i for H = 0.5 m and θ_i for H = 0.03, 1 and 1.5 m. However, even these differences were rather small since they did not exceed 0.018 m^3/m^3. The highest *CV* of θ_i (16.1%) was close to the threshold value (CV = 15%) that discriminates between low and medium variation of a soil property (Warrick, 1998). Consequently, relative variability of θ_i was predominantly small.

Therefore, possible differences between the infiltration runs performed with the six heights of water pouring were not attributable to differences between the antecedent dry soil bulk density and the soil water content of the sampled points since differences between ρ_b and θ_i values were not statistically significant in most cases and practically small to very small in all cases.

Infiltration

Both the cumulative infiltration (I vs. t) and the infiltration rate (i_r vs. I) curves (**Fig. 3**) signaled that the experimental infiltration processes were generally consistent with theory since the concavity of the I vs. t curves was faced downwards and the infiltration rates decreased during the run. In a few cases however, after a quick transient phase, the I vs. t relationship appeared nearly linear, denoting a particularly rapid stabilization of infiltration rates. The mean run duration, d_{tot}, increased monotonically with the height of water pouring from 0.26 h for H = 0.03 m to 1.76 for H = 2 m although it appeared to become nearly stable for $H \geq$ 1.5 m (**Fig. 3**). An infiltration process established with H = 2 m was therefore 6.7

times slower than the one performed with the classical method, that is by applying water at a small distance from the infiltration surface.

The relationships between the mean infiltration time, Δt (h), of a given water volume and the number of the applied water volumes, n_v, revealed differences between the water application heights (**Fig. 4**). In particular, Δt increased with n_v in all cases, according to theory (Elrick and Reynolds, 1992), and also with the height of water pouring starting from the first applied water volume. However, the increase of Δt with H was not continuous since very similar results were obtained for H = 0.03 and 0.25 m on the one hand and for H = 1.5 and 2 m on the other hand, although this last similarity was rather approximate in the final stage of the infiltration process. Therefore, using different heights of water pouring in the range of small H values ($\leq$ 0.25 m) did not affect appreciably infiltration times, that remained small. Increasing H determined a slower infiltration process up to a certain point (H = 1.5 m), beyond which a further increase did not induce an additional slowdown of infiltration. Regardless of H, the experimental data did not describe a clearly horizontal relationship between Δt and n_v at the end of the run, at least with reference to $H \leq 1$ m. This circumstance induced not to exclude a certain overestimation of steady-state infiltration rates from the measured infiltration processes.

For H = 0.25 m, the $\Delta t_H/\Delta t_{0.03}$ ratio varied between 0.85 and 1.30, depending on the applied water volume, and it was on average equal to 1.12 (**Fig. 5**). For the other H values, $1.13 \leq \Delta t_H/\Delta t_{0.03} \leq 9.30$ was obtained. On average, $\Delta t_H/\Delta t_{0.03}$ increased monotonically with H but it appeared to become practically stable for the two highest H values since the mean of $\Delta t_H/\Delta t_{0.03}$ was equal to 6.16 for H = 1.5 m and to 6.21 for H = 2 m. The $\Delta t_H/\Delta t_{0.03}$ ratios increased with the number of the applied water volumes at a different rate, depending on H, but they approached a nearly stable value by the end of the run. In particular, the means of the last five $\Delta t_H/\Delta t_{0.03}$ ratios varied between 1.23 (H = 0.25 m) and 8.04 (H = 2 m) with CVs that did not exceed the 13%.

Therefore, water impact effects: i) started immediately, that is from the first applied water volume, for $H \geq 0.5$ m; ii) increased with the overall applied water amount during the first part of the experiment; and iii) were almost complete, or they continued at an appreciably smaller rate, by the end of the experiment.

In other words, most if not all the possible soil deterioration due to a high height of water pouring occurred by the end of the run. Otherwise, the $\Delta t_H/\Delta t_L$ vs. n_v relationship should have shown a persistent increasing trend also with reference to the applied water volumes in the final phase of the experiment.

Steady-state infiltration rate

For two of the 60 field runs, the Horton model did not yield an estimate of the infiltration parameters. Plotting i_s against i_{fH} did not show any systematic departure from the identity line (**Fig. 6**). The linear regression line between these two variables was statistically significant (coefficient of determination, R^2 = 0.945; $R > 0$; P = 0.05) and the 95% confidence intervals for the intercept and the slope of this linear regression line included zero (from -22.7 to +24.0) and one (from 0.91 to 1.03), respectively, denoting a statistical similarity of the fitted line with the identity one.

Therefore, this analysis suggested a similarity between i_s and i_{fH} and hence it supported the reliability of the estimated i_s and the associated b_s values used in this investigation.

Soil hydraulic properties

The mean values of S decreased as H increased from 0.03 to 2 m (**Table 2**). Numerically, this decrease was not perfectly monotonic since S for H = 2 m was minimally higher, that is by 4%, than S for H = 1.5 m (**Table 2**). Two means of S differed at the most by 2.9 times and

statistically significant differences between the means of S were detected for 11 of the 15 established comparisons. Not significant differences were detected in the range of the smallest H values ($H \leq 0.25$ m) as well as in that of the highest H values ($H \geq 1.5$ m). The CV values of S were higher for $H \leq 0.5$ m (CV = 27-38%) as compared with $H \geq 1$ m (CV = 12-19%). Relative variability was generally medium (Warrick, 1998) with the exception of H = 1.5 m for which variation of S was low.

A similar result was obtained for K_s since this hydrodynamic parameter also decreased almost monotonically as H increased. Even in this case, the only exception was that K_s for H = 2 m was a little greater, that is by 22%, than K_s for H = 1.5 m. Two means of K_s differed up to 18.7 times and differences were statistically significant for 11 comparisons. Even in this case, the smallest H values (≤ 0.25 m) yielded statistically similar results and a statistical similarity was also detected for the largest H values (≥ 1.5 m). The CV values of K_s were higher for $H \leq 0.5$ m (CV = 82-83%) as compared with $H \geq 1$ m (CV = 23-37%). Relative variability of K_s decreased from high to medium with higher H values.

The means of $|h_g|$ increased with H up to H = 0.5 m and then they appeared nearly stable. In this case, two means differed by no more than 1.5 times and differences were statistically significant for only five of the 15 established comparisons. Relative variability of $|h_g|$ was medium regardless of H. Even in this case, the runs performed with the smallest H values yielded the highest CVs. The decrease of CV with H was continuous up to H = 1.5 m because relative variability of $|h_g|$ increased for H = 2 m.

The means of λ_m decreased with H up to H = 0.5 m and then they apparently stabilized. Two means differed by 1.7 times at the most and the differences were statistically significant in only four cases. Relative variability of λ_m was high for H = 0.03 m and medium in the other cases. Also in this case, the decrease of CV with H was monotonic up to H = 1.5 m since relative variability of λ_m increased for H = 2 m.

The S, K_s, $|h_g|$ and λ_m vs. H relationships were statistically significant ($R > 0$) and signaled that S, K_s and λ_m decreased as H increased whereas $|h_g|$ increased (**Fig. 7**). The fitted relationships for S and K_s (R^2 = 0.64-0.66) were stronger than those for $|h_g|$ and λ_m (R^2 = 0.18).

Therefore, the height of water pouring influenced determination of S, K_s, $|h_g|$ and λ_m but the height effects differed with the considered parameter. In particular, S and K_s were overall more sensitive to H than $|h_g|$ and λ_m since, in the former case, more statistically significant differences were detected (**Table 2**) and the relationship with H was stronger (**Fig. 7**). The decrease of S and K_s with H was rather gradual in the range of the tested H values since, in both cases, the two hydrodynamic parameters exhibited high and similar values for the two smallest H values ($H \leq 0.25$ m), they overall decreased as H increased and finally they nearly stabilized for the two highest H values ($H \geq 1.5$ m). Instead, changes in $|h_g|$ and λ_m were appreciable in the range of the smallest H values ($H \leq 0.5$ m in this case) but these two parameters stabilized soon since changes were not significant in the rather wide $0.5 \leq H \leq 2$ m range. Regardless of the considered parameter, using larger H values for the beerkan experiment implied obtaining less variable estimates of the considered parameters. However, there were weak and not statistically supported signs of a reversal of this general trend in the range of the highest H values since the results obtained with H = 2 m were a little higher (S, K_s, λ_m) or lower ($|h_g|$) and more variable than those obtained with H = 1.5 m.

DISCUSSION

In this investigation, higher heights of water pouring generally induced a slowdown of the infiltration process (**Fig. 4**), smaller S, K_s and λ_m values and higher $|h_g|$ values (**Table 2**).

Interpreting the *H* effect as a consequence of spatial variability of soil hydrodynamic properties (e.g., Logsdon and Jaynes, 1996; Popolizio et al., 2022) did not appear convincing since, for each height of water pouring, the experiment was replicated 10 times at randomly selected sampling points within an overall small area (Reynolds et al., 2002). Consequently, it cannot be suggested with a certain confidence that larger heights of water pouring were used in sampling points inherently characterized by a reduced ability to transport water.

Not even the results appeared due to soil slaking although this phenomenon, that induces a sudden soil alteration, can be expected to occur when a nearly dry soil is rapidly wetted (Le Bissonnais, 1996; Martínez-Mena et al., 1998). The reason was that the rapidity with which the soil was wetted did not vary with *H*. In other words, there were not infiltration runs that were performed with an initially slow wetting of the soil and other runs in which initial wetting was fast. Instead, soil wetting was rather fast in all cases meaning that slaking, if it occurred, influenced all infiltration runs performed in this investigation, regardless of *H*.

Therefore, the detected height effects, that confirmed previous findings (Bagarello et al., 2014a, 2023; Alagna et al., 2018; Auteri et al., 2020; Castellini et al., 2021a), likely occurred because more energy was dissipated at the infiltration surface with higher heights. The upper soil layer was altered more appreciably with higher heights of water pouring since dissipating more energy at the soil surface is expected to induce soil compaction and mechanical breakdown (Smith et al., 1990; Le Bissonnais, 1996; Auteri et al., 2020). Consequently, infiltration was hampered (Thompson and Jaynes, 1985; Smith et al., 1990; Assouline and Mualem, 2002; Todisco et al., 2023). More energy implied forming a soil that was overall less sorptive and less conductive and also more homogeneous, in accordance with other investigations (Assouline and Mualem, 2002; Bagarello et al., 2023).

This was the first time that a relatively large number of *H* values were used in a single experiment and this choice made it possible to detect a double threshold mechanism. In particular, height effects can be expected to be small or negligible for both small ($H \leq 0.25$ m) and large ($H \geq 1.5$ m) heights of water pouring. In the former case, a plausible reason is that the soil effectively resisted external solicitations or that, in other terms, these solicitations were not strong enough to alter the soil. In the latter case, the explanation could be that all the possible deterioration occurred with a given height of water pouring and additional solicitations induced with higher *H* values did not further alter the soil. Between these two extremes, the soil degraded with larger heights of water pouring since the external solicitations were high enough to overcome the resistance of the porous medium but not so high as to determine a complete alteration.

An infiltration process that does not depend, or weakly depends, on *H* for small heights of water pouring and then slows down when higher heights are employed for the beerkan run suggested that there was a threshold height which had to be overcome for deterioration processes to be activated. Occurrence of soil alteration only from a certain point on is documented in the literature. For example, Le Bissonnais (1996) stated that mechanical breakdown of aggregates by raindrop impact usually occurs if the kinetic energy of raindrops is great enough. According to Salles et al. (2000), a critical kinetic energy must be reached to initiate soil detachment. An and Liu (2017) reported that collapse of soil aggregates of a given size range depended on the wetting rate. Armenise et al. (2018) recognized the existence of a soil-specific raindrop impact threshold that has to be overcome in order to initiate and support soil detachment.

At the other extreme, an infiltration process that did not depend, or weakly depends, on *H* for large heights of water pouring suggested that there was also a threshold height beyond which deterioration did not develop further. Even the fact that soil alteration does not proceed indefinitely is documented in the literature. For example, Tackett and Pearson (1965) reported that maximum compaction was attained after applying a given amount of rainfall whereas

Roth and Helming (1992) noticed that splash rates as a function of rainfall energy indicated a distinct maximum before leveling off, while both runoff and soil loss displayed asymptotic curves. Detection of an upper threshold H value beyond which soil infiltration did not change further reinforced the suggestion by Auteri et al. (2020) and Bagarello et al. (2023) that the beerkan experiment could be adapted to capture the soil response in the most favorable conditions to runoff occurrence.

In any case, it cannot be omitted that, in this experiment, there was some sign that using H = 2 m instead of H = 1.5 m implied more relative variability of the soil parameters, larger S, K_s and λ_m values and smaller $|h_g|$ values. Although these signs were overall weak and not statistically significant, they could be expressive of the circumstance that, at a certain point, the exclusively or predominantly destructive effect of the applied water ceased and a greater solicitation was less effective than a smaller solicitation in reducing infiltration. This interpretation is not novel since Neave and Rayburg (2007) concluded that seal development will always represent a balance between processes that promote seals and those that actively disrupt seals. In other terms, water impact on the soil surface can be both a formative and a disruptive agent in the process of seal development.

Both S and K_s decreased gradually as H increased and they became nearly stable for $H \geq 1.5$ m. Instead, $|h_g|$ and λ_m were nearly constant for $H \geq 0.5$ m (**Table 2**). Attempting to understand what information was contained in these results, it was considered that: i) S and K_s are linked to each other since soil sorptivity depends, in addition to soil capillarity representing the driving force, on soil hydraulic conductivity that expresses the dissipation (Stewart et al., 2013); ii) the higher $|h_g|$ the smaller the representative pore diameter. Larger $|h_g|$ values in fine soils as compared with coarse soils can be recognized by comparing different investigations (Lassabatere et al., 2006; Nasta et al., 2012; Coutinho et al., 2016) and a tendency of $|h_g|$ to increase with more clay was reported by Bagarello et al. (2014a) and Castellini et al. (2016). The increase of $|h_g|$ in more compacted and disturbed soil conditions was documented, for example, by Mahmoodlu et al. (2016), Bagarello et al. (2020) and Ngo-Cong et al. (2021); iii) the λ_m value represents an effective equivalent mean radius of the pores that participate in the infiltration process (Reynolds et al., 1995; Iovino et al., 2016). The larger λ_m the greater the effect of gravity compared to capillarity as the infiltration driving force (Ndiaye et al., 2005; Souza et al., 2014), and iv) according to Reynolds et al. (1995), K_s depends on both λ_m and the concentration of λ_m pores, N_0 (number of pores/m^2). For a given K_s value, a small λ_m value is compensated by a large N_0 value and vice versa (Castellini et al., 2020). Based on all of this, it appears that, for small H values ($\leq$ 0.5 m), S and K_s decreased as H increased since the soil became more compact (higher values of $|h_g|$) and the effective equivalent mean radius of the pores that participate in the infiltration process, λ_m, became smaller. The decrease of S and K_s that continued to occur as H increased further was likely due to the circumstance that the concentration of λ_m pores became smaller with a higher height of water pouring.

A drawback of the experimental method applied in this investigation was that dry soil bulk density, used to estimate θ_s, was measured by sampling an undisturbed soil, regardless of the used height of water pouring. Therefore, all disturbance effects were captured by the infiltration run but not by ρ_b. Dry soil bulk density is expected to influence the saturated soil hydrodynamic parameters (Assouline, 2006; Ngo-Cong et al., 2021). Therefore, in the future, the experiment should also include sampling the wetted soil volume after the infiltration run for determining the actual ρ_b value. Even better would be to have independent measurements of θ_s at both the beginning and the end of the infiltration run.

Another point to be discussed is that this investigation did not help to establish if total gravitational potential energy, E_p, of the applied water volume can be used to predict variations of soil hydrodynamic properties. Energy depends on both H and the mass of water used for the run (Auteri et al., 2020), which means that the same E_p value could be obtained with different water volumes and heights of water pouring. However, only H was allowed to vary in this investigation. Bagarello et al. (2023) and Agosta et al. (2023) have recently suggested that the hydrodynamic response of a disturbed soil may depend more on the fact that the soil was altered by wetting than on the particular mechanism that causes alteration. Therefore, confidently using E_p for predictive purposes requires preliminarily confirming that a high run with a small water volume and a low run with a large water volume have a similar effect on the soil hydrodynamic response.

Finally, the choice to use six different H values was very appropriate to capture height effects that were not detected before since previous investigations made use of two or three heights of water pouring (e.g., Bagarello et al., 2014a; Auteri et al., 2020; Castellini et al., 2021a). The data obtained in this investigation suggested that, in the future, it could be advisable to use even more H values. In particular, the range of H should be wider, by adding at least one or two H values > 2 m, to verify if the weak signs of a reversal of the soil hydrodynamic response for high H values perceived in this investigation may find a stronger support.

CONCLUSIONS

Compared to the classical beerkan experiment, the multi-height beerkan (MHB) method, i.e., a set of infiltration runs in which water is poured by different heights, should allow to capture the effect of mechanical impact of the applied water on the soil surface, potentially allowing to obtain a more realistic soil hydraulic characterization for simulating hydrological processes.

In this investigation, higher heights of water pouring generally induced a slowdown of the infiltration process, smaller S, K_s and λ_m values and higher $|h_g|$ values. The S, K_s, $|h_g|$ and λ_m vs. H relationships were statistically significant but the fitted relationships for S and K_s were stronger than those for $|h_g|$ and λ_m, thus indicating a different sensitivity of the considered parameters to the height of water pouring.

The relatively large number of H values that was used for the first time in this investigation made it possible to detect a double threshold mechanism. Small or negligible H effects observed for small ($H \leq 0.25$ m) heights of water pouring suggested that there was a threshold height which had to be overcome for deterioration processes to be activated. Small or negligible effects observed for large ($H \geq 1.5$ m) heights suggested that there was also a threshold height beyond which deterioration did not develop further. Between these two extremes, the soil degraded with larger heights of water pouring since the external solicitations were high enough to overcome the resistance of the porous medium but not so high to determine a complete alteration.

Regardless of the water pouring height, the usual beekan runs with fifteen water volumes was adequate to reach near steady-state water flow conditions. The MHB method with six different H values was therefore very appropriate to capture the influence of water impact on the soil surface hydraulic properties that were not detected before using only two or three heights of water pouring.

Future investigations will be aimed at evaluating i) the role of actual surface bulk density that was not measured in this study after the infiltration run and, ii) the role of total gravitational potential energy of the applied water volume in explaining the observed variations of soil hydrodynamic properties. It could be also advisable to consider higher H values, to verify if

the weak signs of a reversal of the soil hydrodynamic response observed for H = 2 m in this investigation may find a stronger support.

CRediT authorship contribution statement

M. Castellini: Conceptualization, Methodology, Investigation, Data curation, Formal analysis, Writing – original draft, Writing – review & editing. **V. Bagarello:** Conceptualization, Methodology, Formal analysis, Writing – original draft, Writing – review & editing. **M. Iovino:** Conceptualization, Methodology, Formal analysis, Writing – review & editing.

Declaration of Competing Interest

The authors declare that they have no known competing financial interests or personal relationships that could have appeared to influence the work reported in this paper.

Data availability

Data will be made available on request.

Acknowledgements

The authors want to thank Luisa Giglio and Antonio Preite for their support during field tests. This study was carried out within the RETURN Extended Partnership and received funding from the European Union Next-GenerationEU (National Recovery and Resilience Plan – NRRP, Mission 4, Component 2, Investment 1.3 – D.D. 1243 2/8/2022, PE0000005), and was supported by the PRIMA Fundation, call 2019-Section 1–GA n.1912 "Research-based participatory approaches for adopting Conservation Agriculture in the Mediterranean Area – CAMA" project.

REFERENCES

Agosta, M., Alagna, V., Bagarello, V., Caltabellotta, G., Iovino, M., Vaccaro, G., 2023. Hydrodynamic response of a loam soil after wetting with different methods. J. Hydrol. 623, 129770, 11 pp., https://doi.org/10.1016/j.jhydrol.2023.129770.

Alagna, V., Bagarello, V., Cecere, N., Concialdi, P., Iovino, M., 2018. A test of water pouring height and run intermittence effects on single-ring infiltration rates. Hydrol. Process. 32, 3793–3804. https://doi.org/10.1002/hyp.13290.

An, J., Liu Q., 2017. Soil aggregate breakdown in response to wetting rate during the inter-rill and rill stages of erosion in a contour ridge system. Catena 157, 241-249, https://doi.org/10.1016/j.catena.2017.05.027.

Armenise, E., Simmons, R.W., Ahn, S., Garbout, A., Doerr, S.H., Mooney, S.J., Sturrock, C.J., Ritz, K., 2018. Soil seal development under simulated rainfall: Structural, physical and hydrological dynamics. J. Hydrol. 556, 211-219, https://doi.org/10.1016/j.jhydrol.2017.10.073.

Assouline, S., Mualem, Y., 2002. Infiltration during soil sealing: The effect of areal heterogeneity of soil hydraulic properties. Water Resour. Res. 38 (12), 1286. https://doi.org/10.1029/2001WR001168.

Assouline, S., Mualem, Y., 2006. Runoff from heterogeneous small bare catchments during soil surface sealing. Water Resour. Res. 42 (12), W12405. https://doi.org/10.1029/2005WR004592.

Auteri, N., Bagarello, V., Concialdi, P., Iovino, M., 2020. Testing an adapted beerkan infiltration run for a hydrologically relevant soil hydraulic characterization. J. Hydrol. 584, 9. https://doi.org/10.1016/j.jhydrol.2020.124697.

Bagarello, V., Castellini, M., Di Prima, S., Iovino, M., 2014a. Soil hydraulic properties determined by infiltration experiments and different heights of water pouring. Geoderma 213, 492–501. https://doi.org/10.1016/j.geoderma.2013.08.032.

Bagarello, V., Di Prima, S., Iovino, M., 2014b. Comparing alternative algorithms to analyze the beerkan infiltration experiment. Soil Sci. Soc. Am. J. 78, 724–736. https://doi.org/10.2136/sssaj2013.06.0231.

Bagarello, V., Cecere, N., David, S.M., Di Prima, S., 2020. Determining short-term changes in the hydraulic properties of a sandy-loam soil by a three-run infiltration experiment. Hydrolog. Sci. J. 65 (7), 1191-1203, https://doi.org/10.1080/02626667.2020.1735637.

Bagarello, V., Caltabellotta, G., Concialdi, P., Iovino, M., 2023. Comparing two methods to perform a beerkan infiltration run in a loam soil at different dates. Journal of Hydrology 617, 129095. https://doi.org/10.1016/j.jhydrol.2023.129095.

Castellini, M., Iovino, M., Pirastru, M., Niedda, M., Bagarello, V., 2016. Use of BEST procedure to assess soil physical quality in the Baratz Lake catchment (Sardinia, Italy). Soil Sci. Soc. Am. J. 80, 742–755.

Castellini, M., Stellacci, A.M., Mastrangelo, M., Caputo, F., Manici, L.M., 2020. Estimating the soil hydraulic functions of some olive orchards: Soil management implications for water saving in soils of Salento peninsula (southern Italy). Agronomy, 10(2):177. https://doi.org/10.3390/agronomy10020177.

Castellini, M., Stellacci, A.M., Di Prima, S., Iovino, M., Bagarello, V., 2021a. Improved Beerkan run methodology to assess water impact effects on infiltration and hydraulic properties of a loam soil under conventional- and no-tillage. Soil Sci. Soc. Am. J. 85, 235–248. https://doi.org/10.1002/saj2.201911.

Castellini, M., Stellacci, A.M., Sisto, D., Iovino, M., 2021b. The mechanical impact of water affected the soil physical quality of a loam soil under minimum tillage and no-tillage: an assessment using Beerkan multi-height runs and BEST-procedure. Land 10, 195. https://doi.org/10.3390/land10020195.

Chen, L., Sela, S., Svoray, T., Assouline, S., 2013. The role of soil-surface sealing, microtopography, and vegetation patches in rainfall–runoff processes in semiarid areas. Water Resour. Res. 49 (9), 5585–5599. https://doi.org/10.1002/wrcr.20360.

Coutinho, A.P., Lassabatere. L., Montenegro, S., Antonino, A.C.D., Angulo-Jaramillo, R., Cabral, J.J.S.P., 2016. Hydraulic characterization and hydrological behaviour of a pilot permeable pavement in an urban centre, Brazil. Hydrol. Process. 30, 4242-4254, https://doi.org/10.1002/hyp.10985.

Di Prima, S., Bagarello, V., Lassabatere, L., Angulo-Jaramillo, R., Bautista, I., Burguet, M., Cerdà, A., Iovino, M., Prosdocimi, M., 2017. Comparing Beerkan infiltration tests with rainfall simulation experiments for hydraulic characterization of a sandy-loam soil. Hydrol. Process. 31, 3520–3532, https://doi.org/10.1002/hyp.11273.

Di Prima, S., Concialdi, P., Lassabatere, L., Angulo-Jaramillo, R., Pirastru, M., Cerdà, A., Keesstra, S., 2018. Laboratory testing of Beerkan infiltration experiments for assessing the role of soil sealing on water infiltration. Catena 167, 373-384, https://doi.org/10.1016/j.catena.2018.05.013.

Di Prima, S., Stewart, R.D., Castellini, M., Bagarello, V. Abou Najm, M.R., Pirastru, M., Giadrossich, F., Iovino, M., Angulo-Jaramillo, R., Lassabatere, L., 2020. Estimating the macroscopic capillary length from Beerkan infiltration experiments and its impact on saturated soil hydraulic conductivity predictions. J. Hydrol. 589, 125159, 11 pp., https://doi.org/10.1016/j.jhydrol.2020.125159.

Elrick, D.E., Reynolds, W.D., 1992. Infiltration from constant-head well permeameters and infiltrometers. p.1-24. In G.C. Topp, W.D. Reynolds and R.E. Green (eds.), Advances

in Measurement of Soil Physical Properties: Bringing Theory into Practice, SSSA Special Publication no.30, Madison, WI, USA.
Fohrer, N., Berkenhagen, J., Hecker, J.-M., Rudolph, A., 1999. Changing soil and surface conditions during rainfall: Single rainstorm/subsequent rainstorms. Catena 37 (3–4), 355–375. https://doi.org/10.1016/S0341-8162(99)00026-0.
Glantz S.A. 2012. Primer of Biostatistics. 7th edition. The McGraw-Hill Companies.
Haverkamp, R., Ross, P.J., Smettem, K.R.J., Parlange, J.Y., 1994. Three-dimensional analysis of infiltration from the disc infiltrometer: 2. Physically based infiltration equation. Water Resour. Res. 30 (11), 2931-2935.
Iovino, M., Castellini, M., Bagarello, V., Giordano, G., 2016. Using static and dynamic indicators to evaluate soil physical quality in a Sicilian area. Land Degrad. Dev. 27, 200-210, https://doi.org/10.1002/ldr.2263.
Horton, R.E., 1940. An approach towards a physical interpretation of infiltration capacity. Soil Sci. Soc. Am. Pro. 5, 399-417.
Lassabatere, L., Angulo-Jaramillo, R., Soria Ugalde, J.M., Cuenca, R., Braud, I., Haverkamp, R., 2006. Beerkan estimation of soil transfer parameters through infiltration experiments – BEST. Soil Sci. Soc. Am. J. 70, 521–532. https://doi.org/10.2136/sssaj2005.0026.
Le Bissonnais, Y., 1996. Aggregate stability and assessment of soil crustability and erodibility: I. Theory and methodology. Eur. J. Soil Sci. 47, 425–437, https://doi.org/10.1111/j.1365-2389.1996.tb01843.x
Lee, D.M., Reynolds, W.D., Elrick, D.E., Clothier, B.E., 1985. A comparison of three field methods for measuring saturated hydraulic conductivity. Can. J. Soil Sci. 65, 563-573.
Lilliefors, H.W., 1967. On the Kolmogorov-Smirnov test for normality with mean and variance unknown. J. Am. Stat. Assoc. 62 (318), 399-402, https://doi.org/10.1080/01621459.1967.10482916.
Logsdon, S.D., Jaynes, D.B., 1996. Spatial variability of hydraulic conductivity in a cultivated field at different times. Soil Sci. Soc. Am. J. 60, 703-709.
Mahmoodlu, M.G., Raoof, A., Sweijen, T., van Genuchten, M. Th., 2016. Effects of sand compaction and mixing on pore structure and the unsaturated soil hydraulic properties. Vadose Zone J. 15 (8), 11 pp., https://doi.org/10.2136/vzj2015.10.0136.
Martínez-Mena, M., Williams, A.G., Ternan, J.L., Fitzjohn, C., 1998. Role of antecedent soil water content on aggregates stability in a semi-arid environment. Soil Till. Res. 48, 71-80.
Mubarak, I., Mailhol, J.C., Angulo-Jaramillo, R., Ruelle, P., Boivin, P., Khaledian, M., 2009. Temporal variability in soil hydraulic properties under drip irrigation. Geoderma 150 (1-2), 158-165, https://doi.org/10.1016/j.geoderma.2009.01.022.
Mügler, C., Ribolzi, O., Janeau, J.-L., Rochelle-Newall, E., Latsachack, K., Chanthamousone, T., Viguierd, M., Jardé, E., Henri-Des-Tureauxd, T., Sengtaheuanghoungf, O., Valentin, C., 2019. Experimental and modelling evidence of short-term effect of raindrop impact on hydraulic conductivity and overland flow intensity. J. Hydrol. 570, 401-410, https://doi.org/10.1016/j.jhydrol.2018.12.046.
Nasta, P., Lassabatere, L., Kandelous, M.M., Šimůnek, J., Angulo-Jaramillo, R., 2012. Analysis of the role of tortuosity and infiltration constants in the Beerkan method. Soil Sci. Soc. Am. J. 76 (6), 1999-2005.
Ndiaye, B., Esteves, M., Vandervaere, J.-P., Lapetite, J.-M., Vauclin, M., 2005. Effect of rainfall and tillage direction on the evolution of surface crusts, soil hydraulic properties and runoff generation for a sandy loam soil. J. Hydrol. 307 (1-4), 294-311, https://doi.org/10.1016/j.jhydrol.2004.10.016.
Neave, M., Rayburg, S., 2007. A field investigation into the effects of progressive rainfall-induced soil seal and crust development on runoff and erosion rates: The impact of

surface cover. Geomorphology 87, 378-390, https://doi.org/10.1016/j.geomorph.2006.10.007.
Ngo-Cong, D., Antille, D.L., van Genuchten, M.Th., Nguyen, H.Q., Tekeste, M.Z., Baillie, C.P., Godwin, R.J., 2021. A modeling framework to quantify the effects of compaction on soil water retention and infiltration. Soil Sci. Soc. Am. J., 15 pp., https://doi.org/10.1002/saj2.20328.
Parlange, J. Y., Lisle, I., Braddock, R. D., Smith, R. E., 1982. The three-parameter infiltration equation, Soil Sci. 133, 337-341.
Philip, J. R., 1957. The theory of infiltration: 1. The infiltration equation and its solution. Soil Sci. 83, 345-358.
Popolizio, S., Stellacci, A. M., Giglio, L., Barca, E., Spagnuolo, M., Castellini, M., 2022. Seasonal and soil use dependent variability of physical and hydraulic properties: An assessment under minimum tillage and no-tillage in a long-term experiment in southern Italy. Agronomy, 12, 3142. https://doi.org/10.3390/agronomy12123142.
Reynolds, W.D., Gregorich, E.G., Curnoe, W.E., 1995. Characterisation of water transmission properties in tilled and untilled soils using tension infiltrometers. Soil Till. Res. 33 (2), 117-131.
Reynolds, W.D., Elrick, D.E., Youngs, E.G., 2002. 3.4.3.2.a Single-ring and double- or concentric-ring infiltrometers. p.821-826. In J.H.Dane e G.C.Topp (co-eds.), Methods of Soil Analysis, Part 4, Physical Methods, Number 5 in the Soil Science Society of America Book Series, Soil Science Society of America, Inc., Madison, WI, USA.
Roth, C.H., Helming, K., 1992. Dynamics of surface sealing, runoff formation and interrill soil loss as related to rainfall intensity, microrelief and slope. J. Plant Nutr. Soil. Sc. 155 (3), 209-216, https://doi.org/10.1002/jpln.19921550309.
Salles, C., Poesen, J., Govers, G., 2000. Statistical and physical analysis of soil detachment by raindrop impact: Rain erosivity indices and threshold energy. Water Resour. Res. 36 (9), 2721-2729.
Smith, H.J.C., Levy, G.J., Shainberg, I., 1990. Water-droplet energy and soil amendments: effect on infiltration and erosion. Soil Sci. Soc. Am. J. 54, 1084-1087.
Somaratne, N.M., Smettem, K.R.J., 1993. Effect of cultivation and raindrop impact on the surface hydraulic properties of an Alfisol under wheat. Soil Till. Res. 26 (2), 115-125, https://doi.org/10.1016/0167-1987(93)90038-Q.
Souza, E.S., Antonino, A.C.D., Heck, R.J., Montenegro, S.M.G.L., Lima, J.R.S., Sampaio, E.V.S.B., Angulo-Jaramillo, R., Vauclin, M., 2014. Effect of crusting on the physical and hydraulic properties of a soil cropped with Castor beans (Ricinus communis L.) in the northeastern region of Brazil. Soil Till. Res. 141, 55-61, http://dx.doi.org/10.1016/j.still.2014.04.004.
Stewart, R.D., Rupp, D.E., Abou Najm, M.R., Selker, J.S., 2013. Modeling effect of initial soil moisture on sorptivity and infiltration. Water Resour. Res. 49, 7037-7047, doi: https://doi.org/10.1002/wrcr.20508.
Tackett, J.L., Pearson, R.W., 1965. Some characteristics of soil crust formed by simulated rainfall. Soil Sci. 99, 407-413.
Thompson, A.L., James, L.G., 1985. Water droplet impact and iys effect on infiltration. Trans. ASAE 1506–1510, 1520.
Todisco, F., Vergni, L., Iovino, M., Bagarello, V., 2023. Changes in soil hydrodynamic parameters during intermittent rainfall following tillage. Catena 226.
van Genuchten, M.T., 1980. A closed-form equation for predicting the hydraulic conductivity of unsaturated soils. Soil Sci. Soc. Am. J. 44 (5), 892-898. https://doi.org/10.2136/sssaj1980.03615995004400050002x.

693 Warrick, A.W., 1998. Appendix 1: Spatial Variability. pp. 655-675 in Hillel D.,
694 Environmental Soil Physics, Academic Press, CA, USA, 771 pages, ISBN 0-12-
695 348525-8.
696 White, I., Sully, M.J., 1987. Macroscopic and microscopic capillary length and time scales
697 from field infiltration. Water Resour. Res. 23 (8), 1514-1522.
698 Yilmaz, D., Lassabatere, L., Angulo-Jaramillo, R., Deneele, D., Legret, M., 2010.
699 Hydrodynamic characterization of basic oxygen furnace slag through an adapted BEST
700 method. Vadose Zone J. 9, 1–10.
701
702

Table 1. Summary statistics of the dry soil bulk density, ρ_b, and the initial volumetric soil water content, θ_i, values close to the locations sampled with different heights of water pouring, *H*

Variable	Statistic	H (m)					
		0.03	**0.25**	**0.5**	**1.0**	**1.5**	**2.0**
ρ_b (g/cm^3)	Min	1.218	1.087	1.120	1.150	1.101	1.184
	Max	1.414	1.326	1.358	1.429	1.435	1.398
	Mean	1.265 ab	1.218 a	1.227 ab	1.273 ab	1.271 ab	1.288 b
	CV (%)	4.6	5.7	6.7	7.1	7.9	5.8
θ_i (m^3/m^3)	Min	0.140	0.116	0.163	0.134	0.135	0.129
	Max	0.172	0.189	0.188	0.174	0.169	0.211
	Mean	0.159 a	0.157 ab	0.173 b	0.155 a	0.155 a	0.157 ab
	CV (%)	6.9	15.9	5.1	8.3	7.4	16.1

Min = minimum value; *Max* = maximum value; *CV* = coefficient of variation.
For a given parameter, means in a row followed by the same lowercase letter are not significantly different according to an F test and a two-tailed t test at $P = 0.05$. Means followed by different lowercase letters are significantly different.

Table 2. Summary statistics of the saturated soil sorptivity, *S*, saturated soil hydraulic conductivity, K_s, scale parameter of the water retention curve, $|h_g|$, and characteristic microscopic pore radius, λ_m, values obtained with different heights of water pouring, *H*

Variable	Statistic	H (m)					
		0.03	**0.25**	**0.5**	**1.0**	**1.5**	**2.0**
S ($mm/h^{0.5}$)	Min	62.4	67.4	40.6	35.9	31.2	30.8
	Max	171.1	152.0	129.4	60.0	48.2	51.8
	Mean	116.3 a	106.0 ab	79.0 b	47.2 c	39.5 d	41.0 cd
	CV (%)	32.8	26.6	38.3	17.1	11.9	18.8
K_s (mm/h)	Min	33.9	36.4	13.3	11.2	7.6	8.0
	Max	679.8	454.3	169.2	32.5	18.0	23.1
	Mean	251.5 a	154.7 ab	62.6 b	20.8 c	13.4 d	16.3 cd
	CV (%)	83.3	82.6	82.4	37.0	23.3	30.6
$\|h_g\|$ (mm)	Min	12.2	46.0	87.3	90.2	101.3	68.8
	Max	133.9	162.6	197.1	171.1	178.0	191.1
	Mean	90.2 ab	101.3 ac	136.0 d	128.1 cd	133.1 d	125.1 bcd
	CV (%)	43.0	38.1	24.5	21.7	16.3	29.7
λ_m (mm)	Min	0.041	0.034	0.028	0.032	0.031	0.029
	Max	0.449	0.118	0.062	0.061	0.054	0.080
	Mean	0.071 a	0.058 ab	0.041 c	0.044 abc	0.042 c	0.046 abc
	CV (%)	82.0	44.2	25.3	21.9	15.9	32.8

Min = minimum value; *Max* = maximum value; *CV* = coefficient of variation.
For a given parameter, means in a row followed by the same lowercase letter are not significantly different according to an F test and a two-tailed t test at $P = 0.05$. Means followed by different lowercase letters are significantly different.

Fig. 1. View of the experimental site at the time of the experiment (a) and of the infiltration runs with a height of water pouring of 0.03 m (b), 0.25 m (c), 0.5 m (d), 1 m (e), 1.5 m (f) and 2 m (g)

Fig. 2. Final infiltration rates estimated by two different methods (Horton, linear regression) for an infiltration process with known parameters

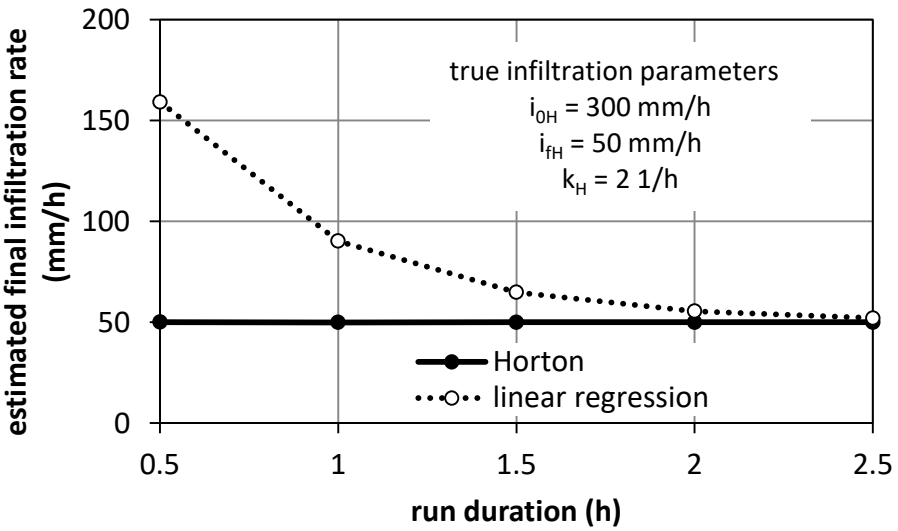

Fig. 3. Cumulative infiltration, I, vs. time, t, and infiltration rate, i_r, vs. I, curves for each height of water pouring (a = 0.03 m; b = 0.25 m; c = 0.5 m; d = 1 m; e = 1.5 m; f = 2 m). The mean infiltration curves (dashed lines) were also reported

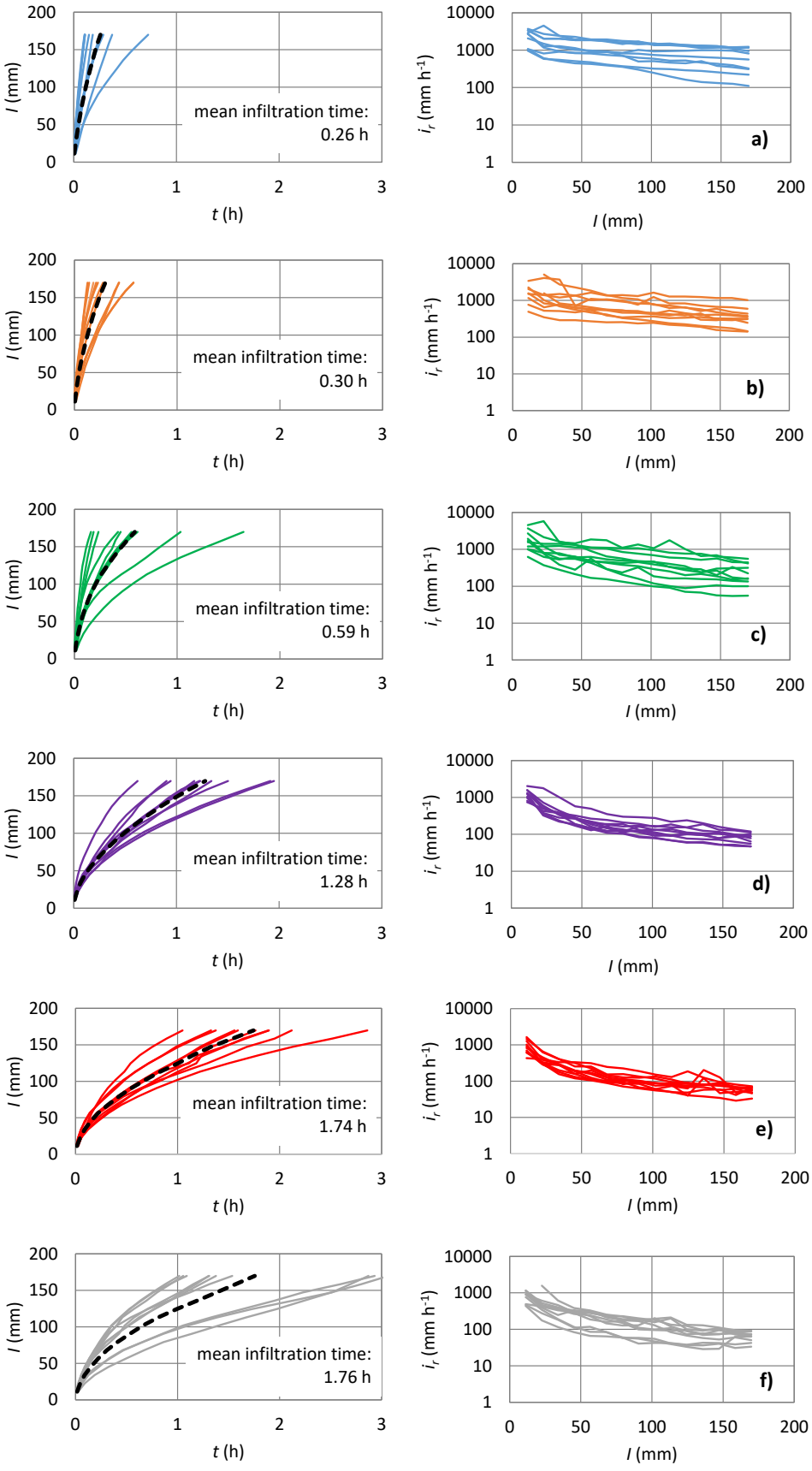

745
746 **Fig. 4.** Means of the infiltration time, Δt, of a given water volume for the runs performed with
747 different heights of water pouring, H
748

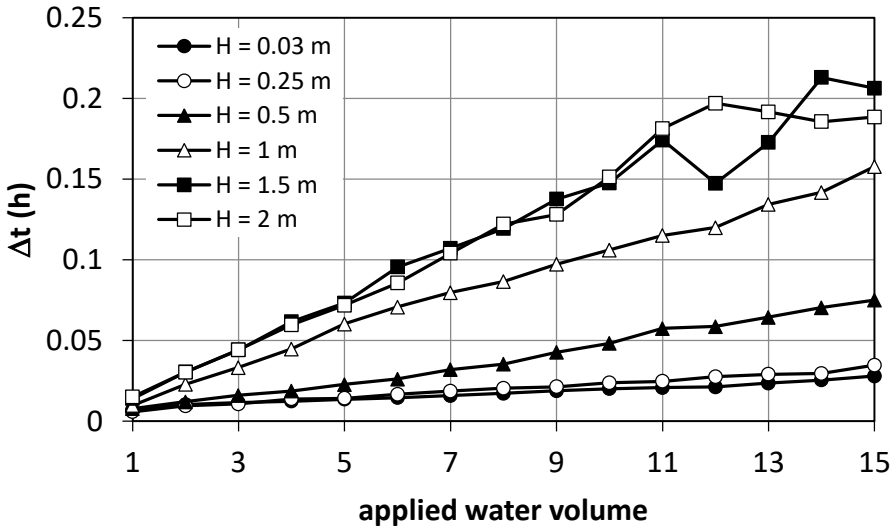

749
750
751
752
753 **Fig. 5.** Ratio between the mean infiltration time for a given height of water pouring, H ($H >$
754 0.03 m), Δt_H, and the mean infiltration time for H = 0.03 m, $\Delta t_{0.03}$, for a given water volume
755

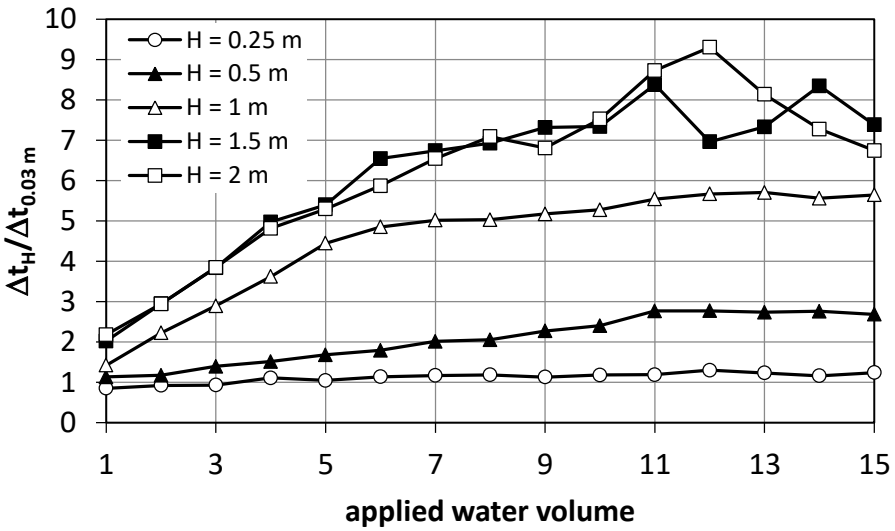

756
757
758
759
760
761
762
763
764

765 **Fig. 6.** Comparison between two estimates of the steady-state infiltration rate for the field
766 runs
767

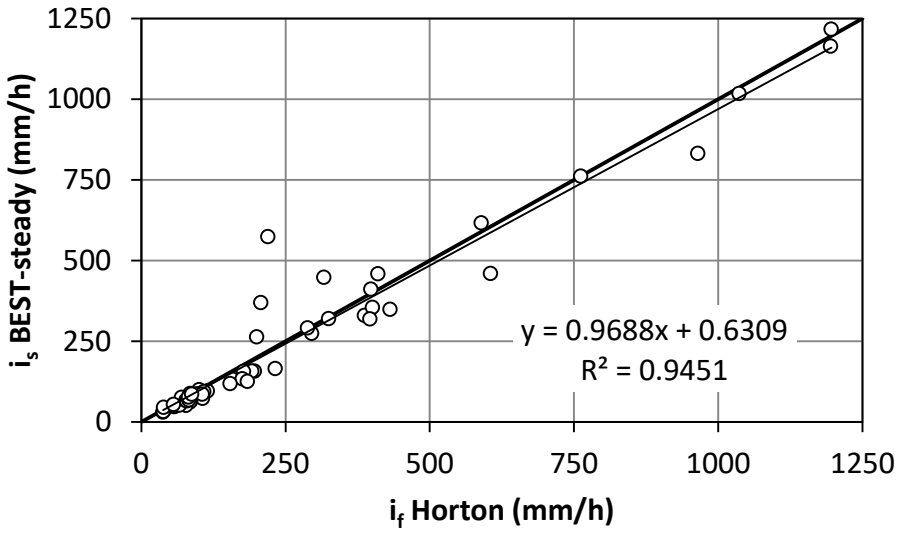

768

Fig. 7. Relationships between the a) saturated soil sorptivity, S, b) saturated soil hydraulic conductivity, K_s, c) scale parameter of the water retention curve, $|h_g|$, and d) characteristic microscopic pore radius, λ_m, values and the height of water pouring, H